We are IntechOpen, the world's leading publisher of Open Access books Built by scientists, for scientists

4,800
Open access books available

122,000
International authors and editors

135M
Downloads

Our authors are among the

154
Countries delivered to

TOP 1%
most cited scientists

12.2%
Contributors from top 500 universities

CLARIVATE ANALYTICS BOOK CITATION INDEX INDEXED

WEB OF SCIENCE™

Selection of our books indexed in the Book Citation Index in Web of Science™ Core Collection (BKCI)

Interested in publishing with us?
Contact book.department@intechopen.com

Numbers displayed above are based on latest data collected.
For more information visit www.intechopen.com

8

Stress Distribution on Edentulous Mandible and Maxilla Rehabilitated by Full-Arch Techniques: A Comparative 3D Finite-Element Approach

Giuseppe Vairo[1], Simone Pastore[2], Michele Di Girolamo[3] and Luigi Baggi[4]

[1]*School of Medical Engineering, University of Rome "Tor Vergata"– Lagrange Laboratory*
[2]*School of Mechanical Engineering, University of Rome "Tor Vergata"*
[3,4]*School of Dentistry, University of Rome "Tor Vergata"*
Italy

1. Introduction

Many surgical protocols and guidelines are actually available in clinical practice for rehabilitating edentulous patients (Bocklage, 2002; Ganeles et al., 2001). They generally differ for number, type, and positioning of implants that support the full-arch prostheses. Moreover, each technique is characterized by a specific healing period and exhibits a success rate strongly affected by individual morphological and biological conditions (Drago, 1992). The actual clinical trend is to reduce both the number of implants and the healing period by employing threaded devices based on novel design concepts, advanced materials, and enhanced surgical procedures. In this context, the immediate-loading techniques, firstly introduced in Seventies, have been recently rediscovered. They usually allow a functional rehabilitation of edentulous arches in a single surgical session, resulting in promising aesthetic and functional results.
Clinical practice confirms that rehabilitation systems based on osseointegrated implants mainly fail because of bone weakening or loss at the peri-implant region rather than as a result of the mechanical failure of the load-bearing prosthetic structure (*e.g.*, Eckert & Wollan, 1998; Lekholm et al., 1999; Piattelli et al., 1996; Romeo et al., 2002; Roos-Jansåker et al., 2006; Tonetti, 1999; Weyant, 2003). Furthermore, the failure rate is generally higher for implants in posterior region than in the anterior (Drago, 1992; Romeo et al., 2002; Roos-Jansåker et al., 2006; Tonetti, 1999; Weyant, 2003), and in maxilla rather than in mandible (Eckert & Wollan, 1998; Lekholm et al., 1999; Piattelli et al., 1996). These evidences, especially in edentulous patients, are strictly related to the poor bone quality and quantity in molar regions, as well as to the different bone density between upper and lower jaws (Devlin et al., 1998). Possible reconstructive alternatives in atrophic cases could be considered (*e.g.*, Keller et al., 1987; Tatum, 1986), but these practices are often characterized by postoperative discomfort, questionable predictability, and surgical complexity (Al-Nawas et al., 2004; Chung et al., 2007). In light of previous considerations and since the presence of sinuses (in maxilla) and mental foramina (in mandible), nowadays full-arch restorations are mainly obtained by placing implants in the anterior region, generally resulting in the use of long cantilevered prostheses.

As pointed out in several researches (*e.g.*, Sertgöz & Güvener, 1996; Shackleton et al., 1994; White et al., 1994), high values of cantilever can be directly associated with high overloading risks. Overloads, generally induced by a shortcoming in load transfer mechanisms under functional forces, lead to possible high stress concentrations at the bone-implant interface, producing in turn possible physiologically-not-admissible strains that activate biological bone resorption (Carter et al., 1996; Guo, 2001; Irving, 1970). As a consequence, cratering phenomena (namely, bone resorption at the implant necks) usually occur, strictly depending on implant geometry and positioning (Baggi et al., 2008a). Recent clinical evidences have showed that such an effect can be minimized by employing microstructured devices subcrestally placed and characterized by a connection diameter of the abutment narrower than the implant collar. These concepts are generally referred to as platform switching (Lazzara & Porter, 2006; Lòpez-Marì et al., 2009; Maeda et al., 2007).

With the aim to reduce cantilever and to obtain a conservative and rational solution for optimizing load transfer mechanisms on the available bone, systems based on tilted implants have been recently proposed (Aparicio et al., 2001; Calandriello & Tomatis, 2005; Capelli et al., 2007; Del Fabbro et al., 2010; Krekmanov et al., 2000; Testori et al., 2008), as well as the possibility to employ short implants in molar regions could be considered (Renouard & Nisand, 2005).

Actually, two of the most used systems for the full-arch immediate-loading rehabilitation of upper and lower edentulous jaws are based on the "Allon4" and "SynCone" concepts (Eccellente et al., 2010; Ferreira et al., 2010; Romanos, 2004). Both systems employ threaded implants usually placed in the anterior region, and allow the functional and aesthetic rehabilitation of 12-14 teeth per arch. The "Allon4" protocol is based on two vertical mesial implants and two tilted distal implants, whose abutments are rigidly fixed to the prosthetic bar. Tilted distal implants are usually distally-angled with respect to the vertical direction of about 30-45 degrees, enabling the use of short cantilevered prostheses. Nevertheless, since in this case implants are crestally positioned, significant cratering effects are generally induced after a healing and functioning period. On the contrary, when "SynCone" protocol is applied, both mesial and distal endosseous implants are conceived on the basis of the platform-switching concepts and are vertically placed. Accordingly, a significant reduction of the crestal bone loss at the implant necks is expected, but a longer cantilever is generally needed for full-arch restorations. In this case the prosthetic denture is retained by telescopic crowns, allowing for excellent three-dimensional immobilization, defined release force, flexibility of design, and optimum access for oral hygiene (Bayer et al., 2009; Wostmann et al., 2007; 2008).

In order to overcome drawbacks of previous rehabilitation systems as well as to account for their advantages, a novel approach is herein proposed and analyzed. It assumes that the prosthetic bar is supported by four vertical implants, designed and positioned in agreement with platform-switching concepts. Two implants are placed in the anterior region and are fully consistent with the SynCone protocol, whereas lateral implants are placed in the posterior molar regions, enabling a significant cantilever reduction (up to zero, if it is possible). Nevertheless, due to the usual quality and quantity of the posterior bone, such a positioning needs the use of short implants (mini implants) similar to those employed in clinical orthodontic or skeletal applications, and sometimes applied in prosthetic dentistry for single-tooth rehabilitations (Baggi et al., 2008a;b; Papadopoulos & Tarawneh, 2007; Renouard & Nisand, 2005).

Clinical effectiveness and reliability of Allon4 and SynCone techniques have been focused in a number of recent studies, showing results of both experimental *in-vivo* tests and follow-up analyses (Degidi & Piattelli, 2005; Ferreira et al., 2010; Khatami & Smith, 2008; Malò et al., 2005; Portmann & Glauser, 2006; Puig, 2010), whereas significant and conclusive clinical evidences are not available for full-arch rehabilitations that combine the use of posterior mini implants and platform-switching concepts.
Nevertheless, clinical *in-vivo* approaches and follow-up analyses usually furnish *a posteriori* indications of functional performance and osseointegration evolution associated with a given rehabilitative protocol. On the contrary, the control *a priori* of design parameters affecting both load transfer mechanisms and possible overloading risks should arise from parametric approaches able to identify stress and strain distributions induced by functional loads. Such a *modus operandi* should allow to obtain clear biomechanical evidences towards the choice of the best treatment in a given clinical scenario, as well as to optimize durability and effectiveness of a specific rehabilitative solution, minimizing patient discomfort and complex clinical procedures.
Stress and strain fields at bone-implant interfaces are affected by a number of biomechanical factors (loading type, material and geometrical properties of both implant and biological *situ*, clinical procedures, Brunski (1997); Mailath-Pokorny & Solar (1996)) and their assessment via *in-vivo* techniques is almost unreliable and ineffective in usual clinical practice (Begg et al., 2009; Clelland et al., 1993). Moreover, the high complexity and the multifield coupling characterizing the bone-implant system generally prevent the use of closed-form approaches. Therefore, numerical methods can be fruitfully employed. In the last years the finite-element method has been widely applied in many fields of dentistry in order to analyze the influence of both mechanical and biological factors, as well as for improving clinical treatments and surgical protocols (*e.g.*, Baggi et al., 2008a;b; Chun et al., 2006; Kitagawa et al., 2005; Maceri et al., 2007; 2009; Petrie & Williams, 2005; Van Staden et al., 2006). In this context, some recent numerical studies have compared the bone-implant mechanical interactions induced by distally-tilted and vertical implants, as well as numerical simulations based on simple geometrical models of Allon4 applications have been carried out (Bellini, 2009; Bonnet et al., 2009; Carvalho Silva et al., 2010; Zampelis et al., 2007). Nevertheless, the numerical analysis of full-arch rehabilitative techniques by using refined three-dimensional models can be still considered at an early stage and then as an actual and open important task.
In this paper the stress-based performances of full-arch rehabiltations supported by four implants and based on the previously-introduced concepts are addressed, by proposing and discussing many numerical results obtained through a three-dimensional finite-element approach. A general numerical method, able to analyze parametrically 3D patient-based models of restored jaws, was developed and applied for comparing three different techniques (namely, Allon4, SynCone-based, and mini-implant-based) when used in both edentulous maxilla and mandible. Load transmission mechanisms and possible bone overloading risks were quantitatively characterized by linearly elastic simulations, considering different functional loads as well as accounting for a detailed and realistic description of both morphological and mechanical aspects.

2. Materials and methods

The following three rehabilitative approaches for the treatment of completely edentulous arches were analyzed and compared:

	ℓ [mm]	d [mm]	p [mm]	t [mm]	L_1 [mm]	L_2 [mm]	c [mm]
SC	9.5 (9.5)	3.5	0.9	0.45	12.0 [16.0]	29.0 [31.0]	15.0
A4	11.0 (15.0)	3.75	0.6	0.2	12.0 [16.0]	35.0 [38.0]	5.0
ZC	9.5 (5.0)	3.5	0.6	0.3	12.0 [16.0]	37.0 [45.0]	0.0

Table 1. Values employed for the main geometrical parameters defining implants and rehabilitative techniques analyzed in this study (SC: SynCone-based, A4: Allon4, ZC: Zero Cantilever). Values of L_1 and L_2 in square brackets refer to mandible model (otherwise in maxilla), and values of ℓ in round brackets refer to distal (posterior in ZC) implants (otherwise mesial). The notation refers to Figs. 1 and 2

- Allon4 (denoted as A4). Full-arch rehabilitations were obtained by four commercially available Nobel Biocare implants (Nobel Biocare AB, Göteborg, Sweden) crestally positioned in the anterior jaw region. Two vertical implants (*i.e.*, with the implant axis orthogonal to the occlusal plane) were placed in the middle part of the anterior jaw region (mesial implants), and two tilted implants in the lateral one (distal implants).
- SynCone-based (denoted as SC). Full-arch rehabilitations were obtained by four (two mesial and two distal) commercially-available Ankylos implants (Dentsply Friadent, Mannheim, Germany), subcrestally and vertically placed in the anterior jaw region.
- Zero Cantilever (denoted as ZC). Full-arch rehabilitations were obtained by: two commercially-available Ankylos implants, placed in the mesial region as in SC; two vertical non-conventional short implants (mini implants, not commercially available), characterized by the Ankylos geometry, and subcrestally placed in the posterior molar region in order to minimize the cantilever.

2.1 Computational models

A trapezoidal thread for all the implants as well as abutments that allow a suitable implant-bar connection were modelled. Abutments of Nobel Biocare implants (in A4) were assumed to be different in vertical and tilted devices, and rigidly connected to the prosthetic bar. Abutments of Ankylos implants (long and short, that is in SC and ZC) were consistent with the platform-switching concepts, and the abutment-bar connection was thought to be achieved by telescopic crowns. In agreement with both commercial availability and clinical practice, numerical models were built up (see Fig. 1) by considering implants whose main geometrical properties are summarized in Table 1.

Implant models were fitted into the computational models of the upper and lower edentulous bone arches (maxilla and mandible). These latter were obtained by disregarding gingival soft tissues and distinguishing between trabecular (inner regions) and cortical (outer layers) bone. The mandible was modelled by considering the complete arch, and temporomandibular joints were accounted for by describing the articular discs as two layer-wise volumes. The maxilla was modelled by reproducing the maxillary process up to the anterior-nasal-spine level, resulting delimited in the upper region by two planar cutting surfaces (Fig. 1).

With the aim to perform significant comparisons, axes of vertical mesial implants were identically positioned for a given jaw in all the three approaches, and implant lengths were chosen such that the in-bone depth was the same, except for the posterior short implants in ZC. Distal implants in A4 were assumed to be distally-tilted at a 30-degree angle in the plane orthogonal to the buccal-lingual direction, and positioned such that their in-bone ends belong

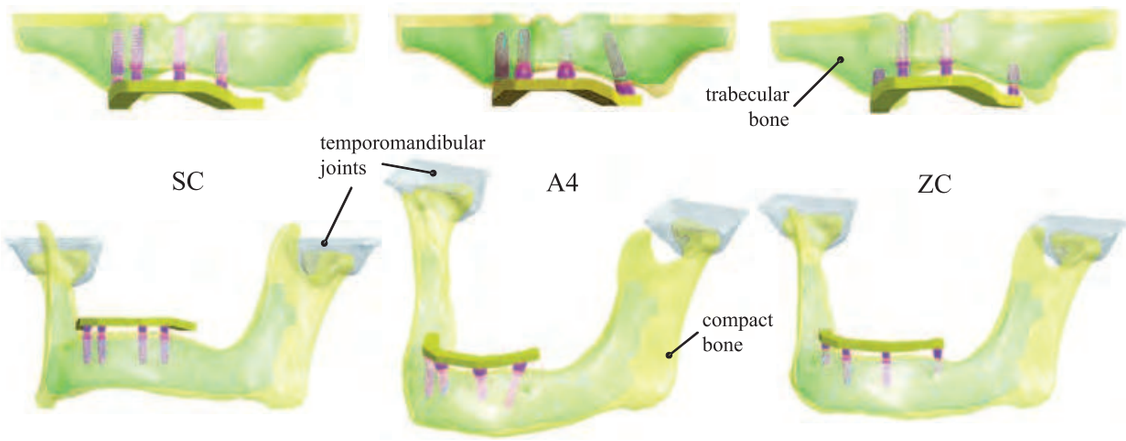

(a) Solid models

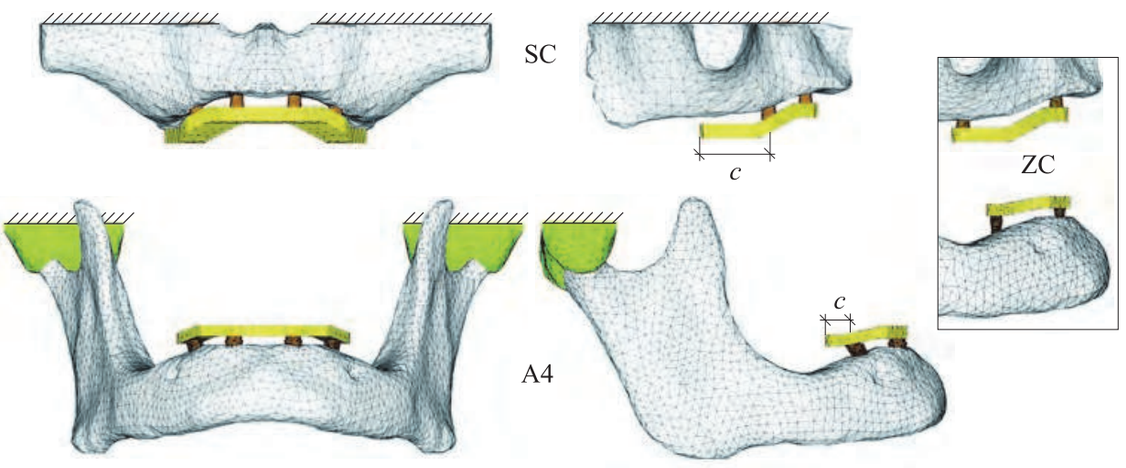

(b) Mesh details

Fig. 1. Three-dimensional computational models for mandible and maxilla equipped with three different rehabilitative devices: SynCone-based (SC), Allon4 (A4) and Zero Cantilever (ZC). As a notation rule, *c* denotes the cantilever length

to the vertical axes of the SC's distal implants (Fig. 2). Accordingly, a cantilever scheme 5 mm long for A4 and 15 mm for SC arose (Fig. 1 and Table 1). For what concerns ZC, posterior mini implants were placed so that a zero cantilever length was obtained. Due to the different bone morphology in lower and upper jaws and in agreement with general clinical guidelines, distances among implants in mandible and maxilla were assumed to be different (Fig. 2 and Table 1).

The prosthetic bar was modelled by considering a pseudo-parabolic middle-line geometry that followed the bone morphology. Implant abutments and bar shape were arranged to ensure that the distance between bar and bone was about 5 mm. The bar, slightly different in shape for mandible and maxilla, was 3 mm thick, 5 mm depth, and its linear length in the occlusal plane was 65.8 mm. It is worth pointing out that the bar's mechanical response was behind the scope of the present study and then the bar modeling has been performed with the only purpose to allow a suitable loading transfer towards the implant-bone coupled system.

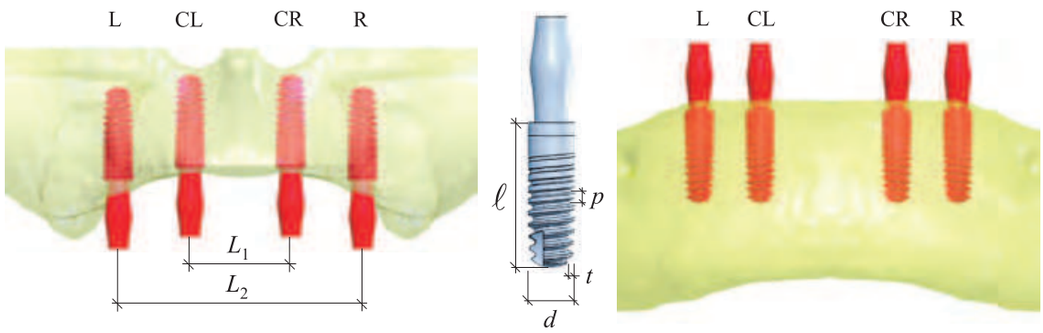

(a) SynCone-based technique (SC) employing Ankylos implants

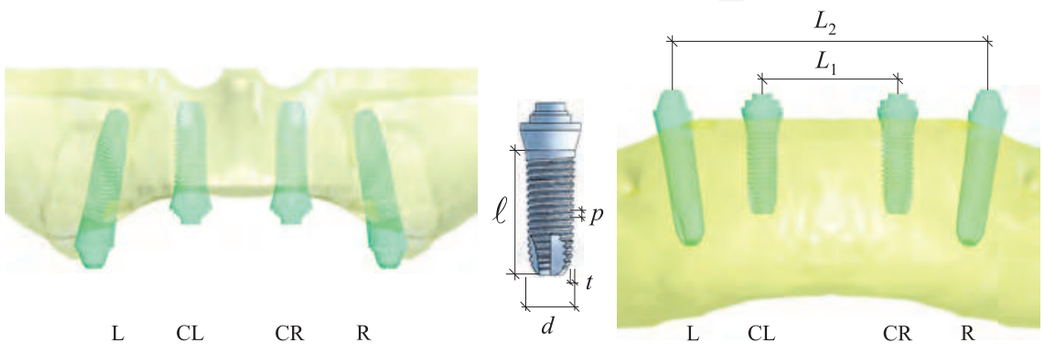

(b) Allon4 technique (A4) employing Nobel Biocare implants

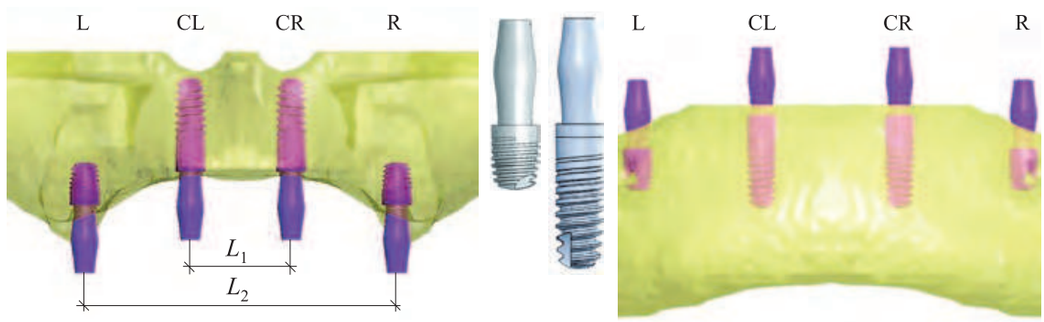

(c) Zero-Cantilever technique (ZC) employing Ankylos implants and Ankylos-type mini implants

Fig. 2. Implant positioning in both edentulous maxilla (on the left) and mandible (on the right). ℓ: implant length; d: implant maximum diameter; p: average thread pitch; t: average thread depth; L_1: distance between mesial implants; L_2: distance between distal implants; L: left implant; CL: central-left implant; CR: central-right implant; R: right implant

In order to describe realistically the physiological structure of the cortical bone arising around a functioning implant after a healing period, different peri-implant crestal bone geometries were modelled, depending on both implant shape and positioning. Starting from the local bone configurations and the virtual implant positioning, Fig. 3 sketches

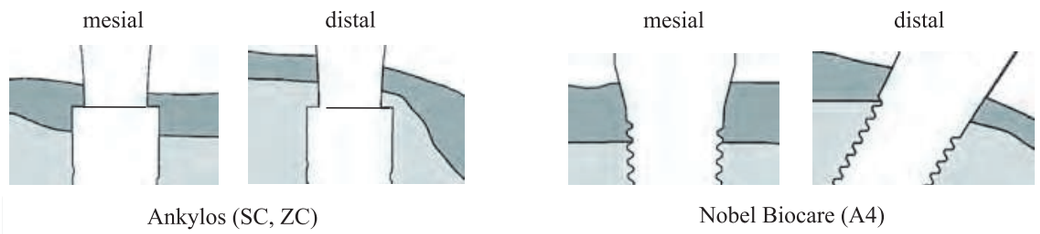

(a) Virtual implant positioning

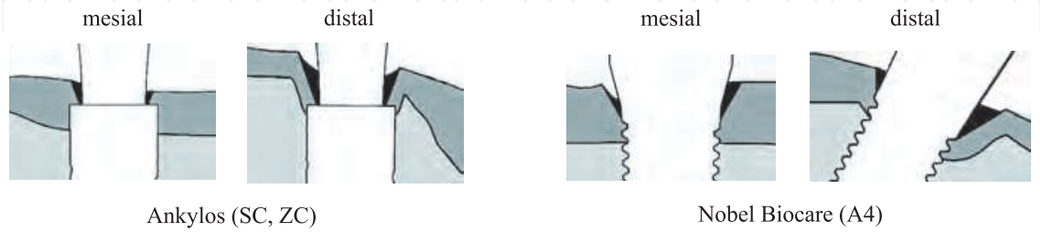

(b) Peri-implant post-healing geometry

Fig. 3. Geometrical modeling of the post-healing crestal bone morphology in functioning implants. Comparison with the local bone configurations obtained after the virtual implant positioning

as the peri-implant bone geometries were arranged in order to match well-established clinical evidences associated with crestal bone loss and remodeling at the implant necks (Abboud et al., 2005; Degidi et al., 2009; Shin et al., 2006). Accordingly, for Nobel Biocare devices the peri-implant cortical geometries were modelled such that the first coil was always in contact with the compact bone layer, and a cratering morphology with a mean crestal bone loss of about 45% in thickness was considered. In the case of Ankylos implants (short and long), since the platform-switching configuration and subcrestal positioning, a lower crestal bone loss (assumed to be about 20% in thickness), and a bone layer apposition (about 0.3 mm thick) were modelled.

Three-dimensional models of implants and prosthetic bar were developed by using a parametric CAD software (SolidWorks 9; Dassault Systems, Concord, Massachusetts). Detailed solid models of mandible and maxilla were built up from patient-based computed tomography images, and morphological parameters were evaluated by using a commercial tool (Mimics 10.1; Materialise Dental NV, Leuven, Belgium). All 3D volumes were arranged by using the CAD software, generating as an output the models fully compatible with a commercial finite-element code (Ansys 11.0; Ansys Inc, Canonsburg, Pa). The latter was used for merging all parts, as well as for generating and solving the discrete numerical models. Computational meshes were obtained by employing ten-node tetrahedral elements based on a classical pure displacement formulation, with quadratic shape functions and three degrees of freedom per node (Zienkiewicz & Taylor, 2005).

As a result of a preliminary convergence analysis, the mean value of the mesh size was set equal to about 1 mm far away from the bone-implant interfaces, and to about 0.1 mm at the peri-implant regions (Fig. 1). In this way, good accuracy and admissible computing effort were obtained, with an expected relative error for the displacement-based numerical solutions less than 0.1% at the peri-implant regions and less than 2% elsewhere (Baggi et al., 2008b;

	SynCone (SC)		Allon4 (A4)		Zero Cantilever (ZC)	
	Mandible	Maxilla	Mandible	Maxilla	Mandible	Maxilla
Nodes	235,465	281,279	263,354	258,780	251,780	254,113
Elements	431,561	449,287	421,220	448,254	432,974	468,423

Table 2. Number of elements and nodes characterizing present convergent finite-element models

Material	Region	E [GPa]	ν
Titanium Alloy[a,b]	Implants	114.0	0.34
Gold Alloy[a,b]	Prosthetic bar	105.0	0.23
Cancellous bone[c,d]	Mandible	1.0	0.3
	Maxilla	0.5	0.3
Cortical Bone[c,d]	Mandible and maxilla	13.7	0.3
Soft tissue[e]	Articular discs (in mandible)	0.006	0.4

[a] Lemon & Dietsh-Misch (2007)
[b] Baggi et al. (2008b)
[c] Natali et al. (2003)
[d] Baggi et al. (2008a)
[e] Beek et al. (2000)

Table 3. Elastic constants adopted in finite-element analyses (E: Young modulus, ν: Poisson ratio)

Zienkiewicz & Zhu, 1987; Zienkiewicz & Taylor, 2005). Table 2 summarizes the number of elements and nodes characterizing the convergent discrete models employed in this study.

2.2 Material properties

Dry material models approximated the biological tissues (that is, bone and articular discs), neglecting any effect of fluid-solid interactions. Materials were assumed to be characterized by a linearly elastic isotropic behavior, and all material volumes were considered as homogeneous. Referring to well-established approaches available in literature (Baggi et al., 2008a;b; Beek et al., 2000; Lemon & Dietsh-Misch, 2007; Natali et al., 2003), Table 3 summarizes the elastic properties adopted in this study.
It is worth pointing out that, according with the classification of Lekholm & Zarb (1985), material properties considered for mandibular tissues approximate a quality-II bone, whereas maxillary trabecular bone was assumed to be less dense than mandible's, resulting in a smaller value of the Young modulus (Beek et al., 2000).

2.3 Loading and Boundary Conditions

Finite-element analyses were carried out considering three different static loading scenarios (Fig. 4):

- Full mouth biting (denoted as Load 1), defined as a uniformly distributed intrusive vertical load acting upon the free surface of the prosthetic bar, with a resultant value of 300 N.

- Cantilever load (Load 2), defined as a distal concentrated load applied at the end of the right cantilever, and angled with reference to the vertical axis. It consists in an intrusive vertical component of 250 N and in an horizontal one (along the buccal-lingual direction) of 100 N.
- Frontal load (Load 3), defined as a concentrated load applied at the midspan of the bar portion between mesial implants, consisting in an intrusive vertical component of 250 N and in an horizontal one (along the buccal-lingual direction) of 100 N.

Muscular forces were disregarded in the case of the maxillary arch and were included in the mandible model. In agreement with Trainor et al. (1995), forces relevant to masseter, temporalis and internal pterygoideus muscles were taken into account, by assuming uniformly distributed loads on the corresponding physiological surfaces (Fig. 5). With reference to the Cartesian frame introduced in Fig. 5 and depending on the loading type, components of the resultant muscular forces produced by these distributions were summarized in Table 4.

For what concerns boundary conditions, complete osseous integration between implants and bone was modelled, resulting in the continuity of displacements at the implant-bone interfaces. Furthermore, displacement functions were assumed to be continuous at all possible interfaces among contiguous volumes. The overall arch models equipped with rehabilitative devices were constrained by preventing any displacement component of every node belonging to the upper surfaces of the layer-wise articular discs in mandible and to the virtual cutting surfaces in maxilla (see Fig. 1).

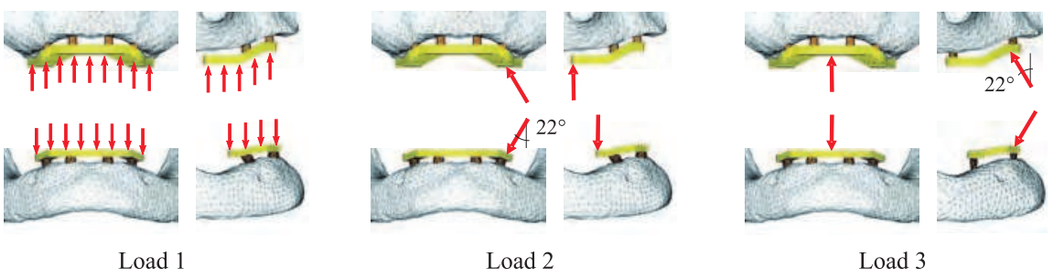

Fig. 4. Loading conditions. Load 1: full mouth biting. Load 2: cantilever load. Load 3: frontal load

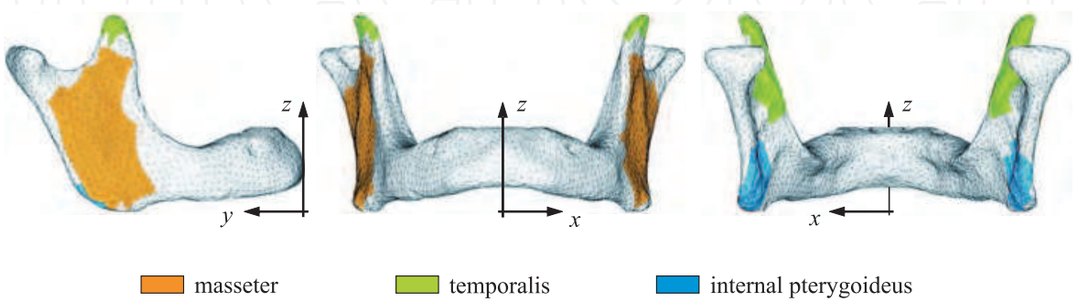

Fig. 5. Physiological surfaces on mandible model where muscular force distributions were assumed to be uniformly applied

	Masseter			Temporalis			Pterygoideus		
Comp.	x	y	z	x	y	z	x	y	z
Load	[N]	[N]	[N]	[N]	[N]	[N]	[N]	[N]	[N]
1	20.0	-31.8	82.8	9.7	19.4	77.8	-20.6	-12.5	35.7
	(-20.0)	(-31.8)	(82.8)	(-9.7)	(19.4)	(77.8)	(20.6)	(-12.5)	35.7
2	20.0	-31.8	82.8	9.7	19.4	77.8	-20.6	-12.5	35.7
	(-13.2)	(-21.0)	(54.6)	(-8.2)	(16.3)	(65.3)	(13.9)	(-8.4)	(24.1)
3	20.9	-33.3	86.6	16.8	33.5	134.1	-19.0	-11.4	32.8
	(-20.9)	(-33.3)	(86.6)	(16.8)	(33.5)	(134.1)	(19.0)	(-11.4)	(32.8)

Table 4. Components of the resultant muscular forces acting upon the mandible model, referred to the Cartesian frame introduced in Fig. 5 and to the loading cases under investigation. Values in (respectively, not in) parentheses indicate force components acting upon the corresponding physiological surfaces at $x > 0$ (respectively, $x < 0$)

2.4 Stress measures, risk indicators, and loading partition index

The models of lower and upper jaws treated by the previously-introduced techniques were numerically analyzed and, in order to furnish risk measures of critical bone overloading as well as performance indications on load transfer features, comparisons were performed evaluating stress distributions on both cancellous and compact bone at the peri-implant regions. In agreement with well-established studies (Baggi et al., 2008a;b; Bellini, 2009; Bonnet et al., 2009; Carvalho Silva et al., 2010; Chun et al., 2006; Kitagawa et al., 2005; Petrie & Williams, 2005; Van Staden et al., 2006; Zampelis et al., 2007), the Von Mises equivalent stress σ_{VM} (always positive in sign) was used as a global stress indicator for characterizing the load transfer mechanisms, whereas principal stresses were employed as local risk measures of the bone-implant interfacial physiological failure and/or of the resorption process activation. Accordingly, by assuming the ultimate bone strength as a physiological limit, local overloading at the cortical bone occurs in compression when the maximum compressive principal stress (σ_C) exceeds 170-190 MPa in modulus, and in tension when the maximum tensile principal stress (σ_T) exceeds 100-130 MPa, as well as local overloading at the trabecular bone occurs when σ_T and/or $\|\sigma_C\|$ exceeds 5 MPa (Guo, 2001; Natali et al., 2003), symbol $\|\sigma_C\|$ denoting the modulus of σ_C.

For each implant mean and peak values of σ_{VM}, σ_C, and σ_T were computed at both trabecular (Σ_t) and compact (Σ_c) peri-implant control volumes, defined by considering bone layers about 1 mm thick surrounding the implants (Baggi et al., 2008b). Stress solutions obtained by 3D finite-element simulations were post-processed through a custom-made procedure, employing as an input some geometric and topological data (namely, nodal coordinates and elements lying in bone-implant interfacial control volumes Σ_t and Σ_c), as well as stress solutions at the Gauss integration points.

In order to analyze quantitatively the loading partition mechanisms in rehabilitative approaches herein investigated, a meaningful performance index was also introduced, denoted in the following as partition ratio. In detail, under an assigned load and for a given bone arch, the partition ratio at the peri-implant bone region r of the implant $\mathcal{I}$ and related to the technique $\mathcal{T}$ was defined as:

$$P_r^{(\mathcal{I},\mathcal{T})} = \frac{(\bar{\sigma}_{VM})_r^{(\mathcal{I},\mathcal{T})}}{(\bar{\sigma}_{VM})_r^{\max}} \tag{1}$$

$(\sigma_{VM})_r$ denoting the average value of the Von Mises stress distribution in Σ_r (with $r = t, c$), and $(\bar{\sigma}_{VM})_r^{\max}$ indicating the maximum value of $(\bar{\sigma}_{VM})_r$ computed for all implants in all rehabilitative techniques, that is

$$(\bar{\sigma}_{VM})_r^{(\mathcal{I},\mathcal{T})} = \frac{1}{(\Sigma_r)^{(\mathcal{I},\mathcal{T})}} \int_{(\Sigma_r)^{(\mathcal{I},\mathcal{T})}} \sigma_{VM}^{(\mathcal{T})} \, d\Sigma \tag{2}$$

$$(\bar{\sigma}_{VM})_r^{\max} = \max_{\mathcal{T}} \left\{ \max_{\mathcal{I}} \left\{ (\bar{\sigma}_{VM})_r^{(\mathcal{I},\mathcal{T})} \right\} \right\} \tag{3}$$

where, in agreement with the notation rules introduced in Fig. 2, $\mathcal{I}$ = L, CL, CR, R and $\mathcal{T}$ = SC, A4, ZC.
Therefore, a prosthetic treatment on a given jaw and for an assigned load can be retained to exhibit load transmission performance better than another one if the corresponding values of P are more uniformly distributed among the supporting implants. Furthermore, small values of P can be retained to furnish a first indication of low overloading risks. Nevertheless, since the Von Mises stress measure does not allow to trace a distinction between tensile and compressive local stresses, more effective and straight evidences on possible overloads were obtained by analyzing stress measures σ_C and σ_T (Baggi et al., 2008a;b).

3. Results

The main findings obtained by numerical simulations are proposed and discussed in the following. Figures 6 and 7 show the Von Mises stress distributions at the peri-implant bone regions in maxilla and mandible, respectively, for the three rehabilitation techniques previously introduced and considering different loads. For a given implant, numerical results have been plotted in the plane containing the implant axis and orthogonal to the buccal-lingual direction. Moreover, in order to obtain significant comparisons, the same contour legend has been employed in all cases. In Fig. 8 values of the partition ratio P, computed in both upper (Fig. 8a) and lower (Fig. 8b) jaw, and for cortical (P_c) and trabecular (P_t) bone regions, are plotted and compared. Finally, Figs. 9 and 10 depict mean (bars) and peak (lines) values of the principal stress measures σ_C and σ_T, computed at each peri-implant cortical (Σ_c, Fig. 9) and trabecular (Σ_t, Fig. 10) bone region of maxilla and mandible.
All the numerical simulations clearly highlighted that stress concentration areas were located at the cortical bone around the implant necks, and that the right cantilever load (namely, Load 2) was the most severe, resulting in the highest values of stresses (both Von Mises and principal measures) at the right peri-implant bone.
For what concerns the comparison between conventional techniques (namely, A4 and SC), Von Mises stress patterns induced by A4-based restorations in both lower and upper jaw were more homogeneous and characterized by smaller stress values than SC, except in the maxillary rehabilitation under the frontal load (Load 3). Such an evidence is fully confirmed by analyzing the values of the partition index P. In fact, for all loading conditions in mandible and for full mouth biting and cantilever load in maxilla, A4 produced more uniform distributions of P among the implants (*i.e.*, better load transmission mechanisms) than SC. On the contrary, when the frontal load was applied on the upper jaw, differences among the values of P at mesial and distal implants were greater in A4 rather than in SC. In mandible, the greatest differences in P between A4 and SC were experienced at the right implant under the Load 2 (P_{A4} was smaller than P_{SC} of about 18% in cortical bone, and 60% in trabecular), and at the distal implants in the case of Load 1 and Load 3 (P_{A4} was smaller than P_{SC} of

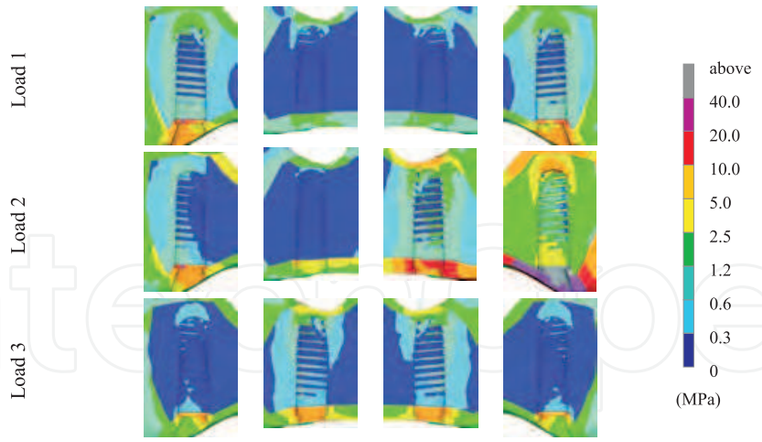

(a) SynCone-based rehabilitation (SC)

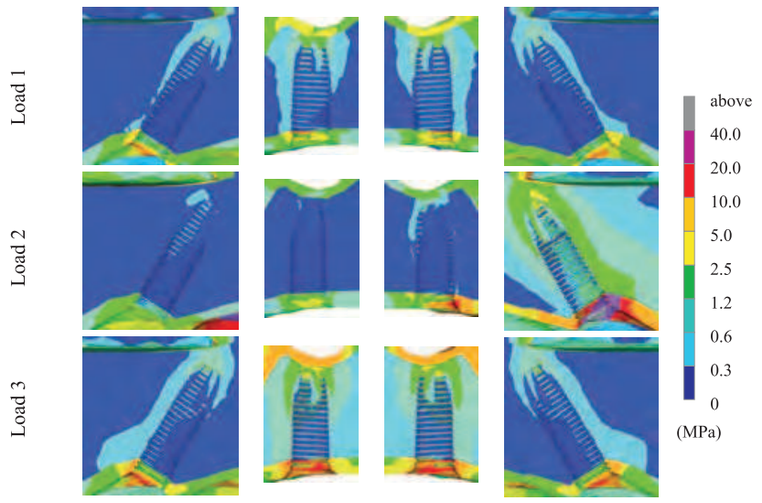

(b) Allon4 rehabilitation (A4)

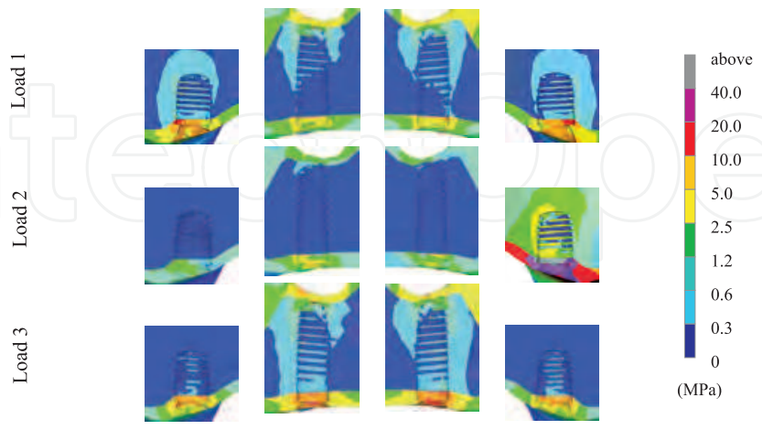

(c) Zero-Cantilever rehabilitation (ZC)

Fig. 6. Von Mises stress contours at each peri-implant bone region in maxilla, referred to the plane containing implant axis and orthogonal to the buccal-lingual direction

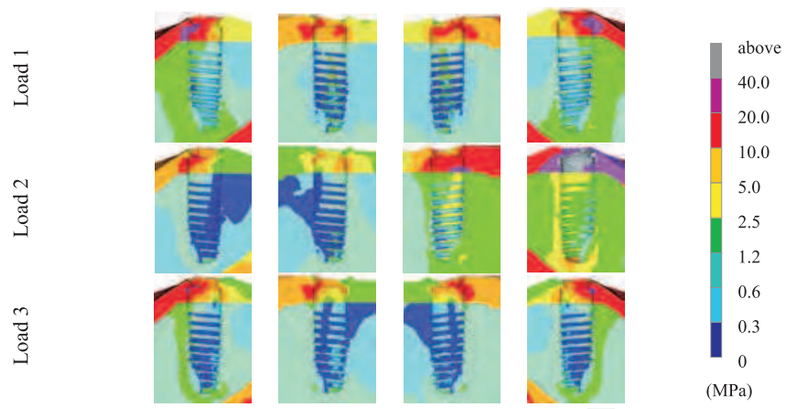

(a) SynCone-based rehabilitation (SC)

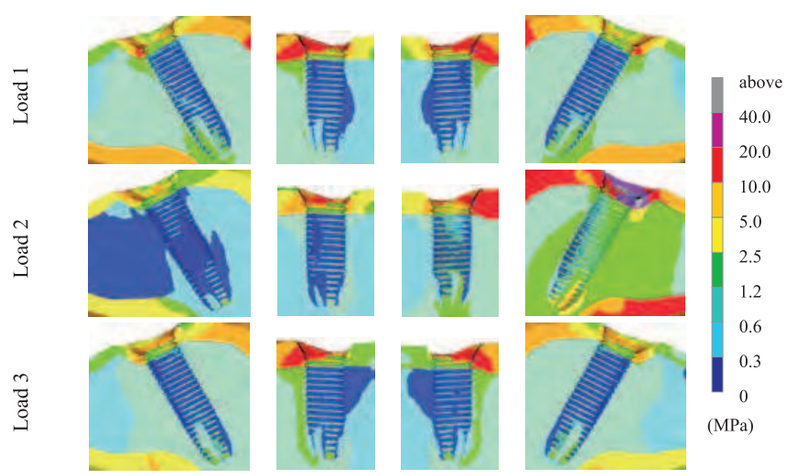

(b) Allon4 rehabilitation (A4)

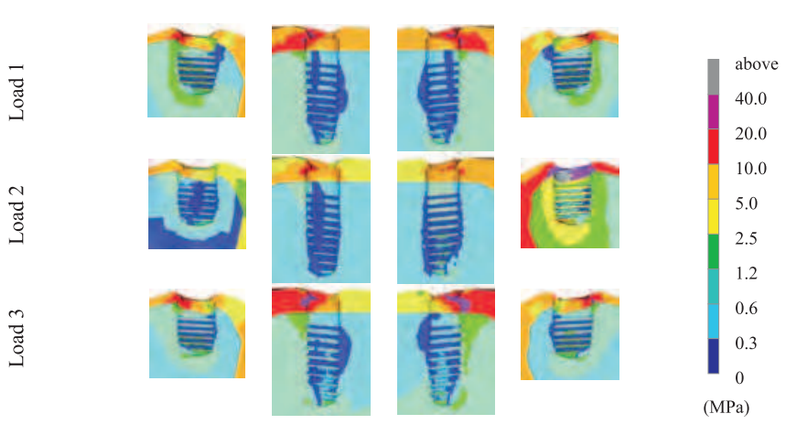

(c) Zero-Cantilever rehabilitation (ZC)

Fig. 7. Von Mises stress contours at each peri-implant bone region in mandible, referred to the plane containing implant axis and orthogonal to the buccal-lingual direction

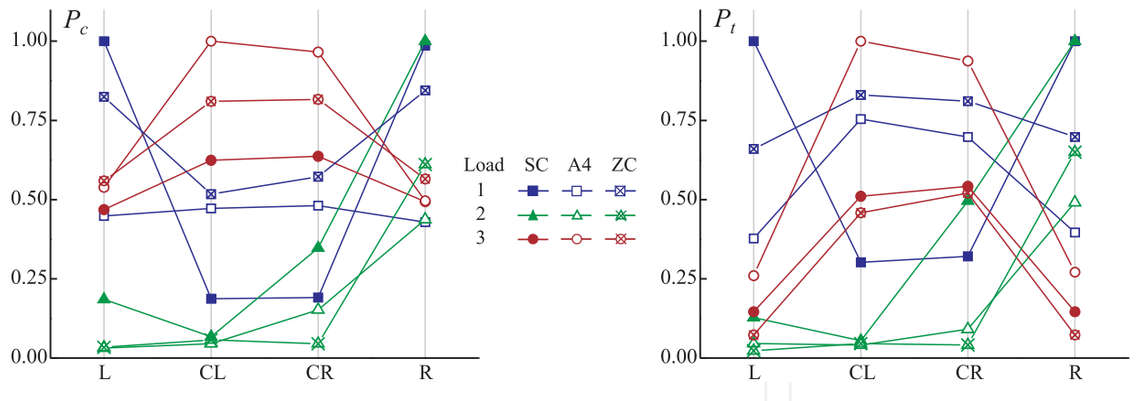

(a) Maxilla

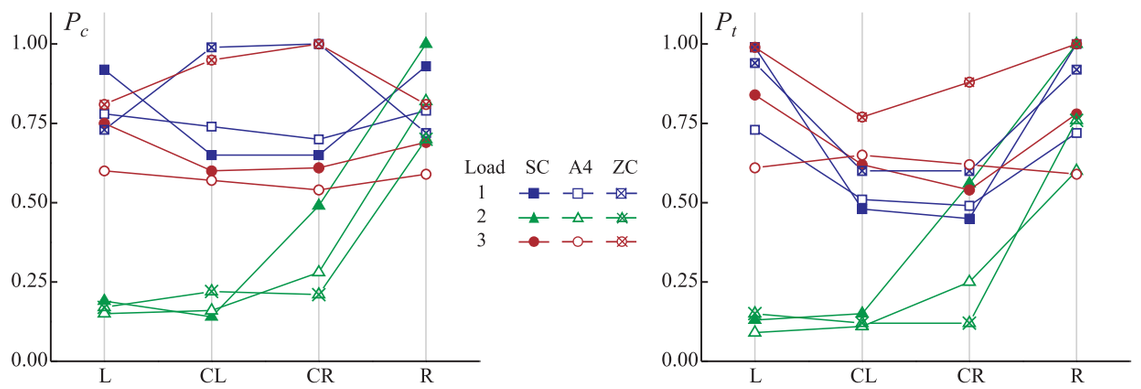

(b) Mandible

Fig. 8. Loading partition ratio at cortical (P_c, on the left) and trabecular (P_t, on the right) bone for SynCone-based (SC, filled symbols), Allon4-based (A4, unfilled symbols), and Zero Cantilever (ZC, cross symbols) rehabilitations, in upper (a) and lower (b) jaw under different loads (Load 1: full mouth biting, blue symbols; Load 2: cantilever load, green symbols; Load 3: frontal load, red symbols; L: left implant; CL: central-left implant; CR: central right implant; R: right implant)

about 15-22% in cortical bone, and about 30% in trabecular). In maxilla and for Load 2, the greatest differences in P were again at the right implant (P_{A4} was smaller than P_{SC} of about 56% in cortical bone, and 51% in trabecular), whereas a different behavior with respect to the mandible was proved under Load 1 and Load 3. In detail, for a full-mouth-biting load applied on the SC-based restoration, distal implants transferred the greatest amount of the load (mesial P_{SC} was smaller than the distal's of about 70-80%), whereas with A4 the load was more uniformly distributed, resulting in greater contributions acting upon the mesial implants (distal P_{A4} was smaller than the mesial's of about 5-10% in cortical bone, and 45-50% in cancellous). On the contrary, for Load 3 acting on the maxillary jaw the system A4 exhibited the worst performance, resulting in values of both P_c and P_t higher and less homogeneous (*e.g.*, the difference between mesial and distal values of $(P_c)_{SC}$ was smaller than $(P_c)_{A4}$ of

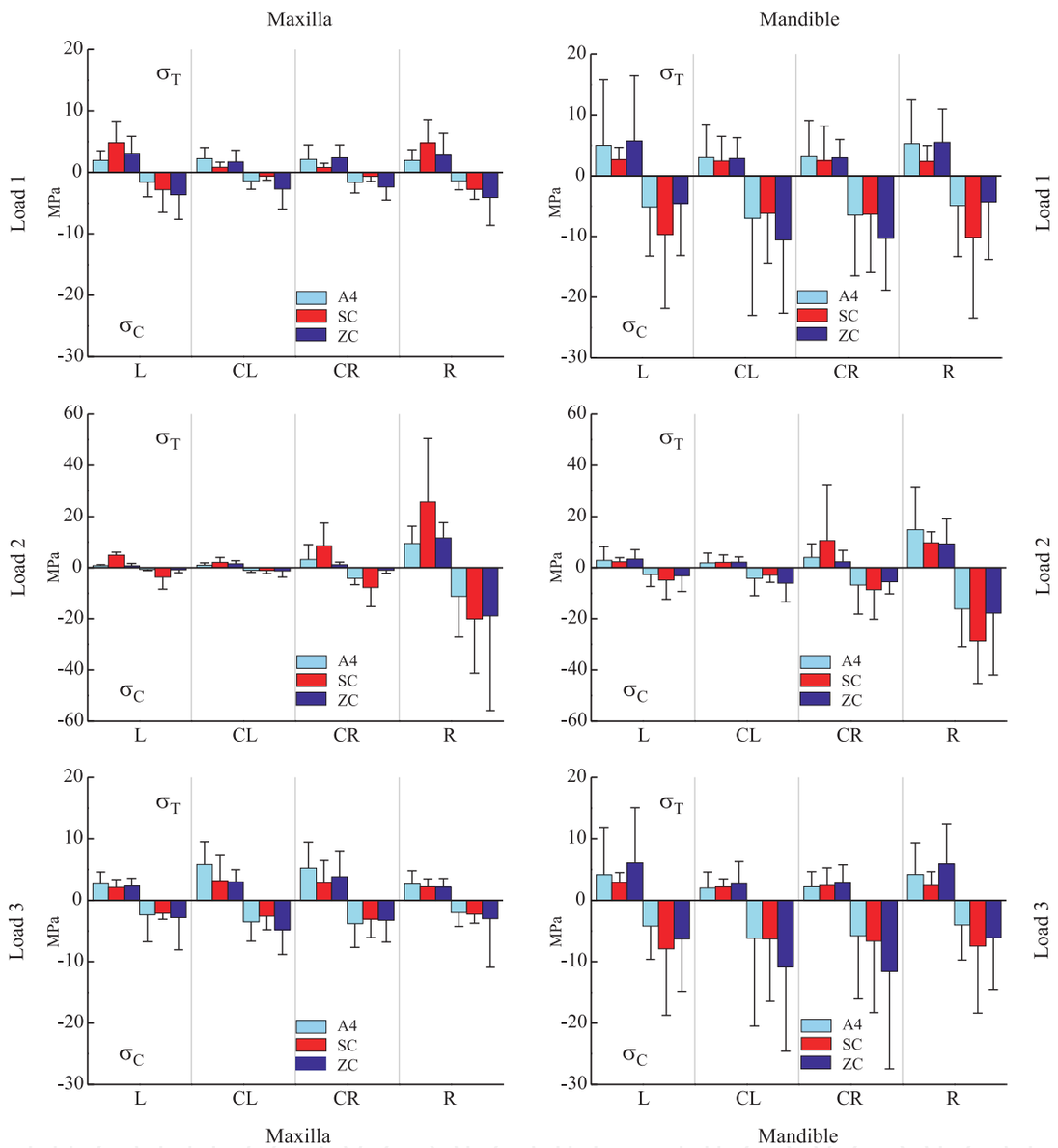

Fig. 9. Principal stress measures (σ_C compressive and σ_T tensile) at the cortical bone-implant interfaces for implants in A4 (Allon4, light blue bars), SC (SynCone-based, red bars), and ZC (Zero Cantilever, violet bars) restorations, in maxilla (on the left) and mandible (on the right). Average (bars) and peak (lines) values (L: left implant; CL: central-left implant; CR: central-right implant; R: right implant)

about 50-60%, with the highest values of $(P_c)_{SC}$ –at the mesial implants– smaller than those of $(P_c)_{A4}$ of about 40-50%).

As regards the non-conventional Zero-Cantilever approach (ZC), it produced Von Mises stress patterns at the peri-implant bone regions very similar in both values and homogeneity levels to those obtained with A4. Moreover, the use of Ankylos-type mini implants at the posterior molar regions allowed to achieve loading partition mechanisms almost comparable (sometimes better, as for Load 2 in mandible) with those obtained through both A4 and SC. In

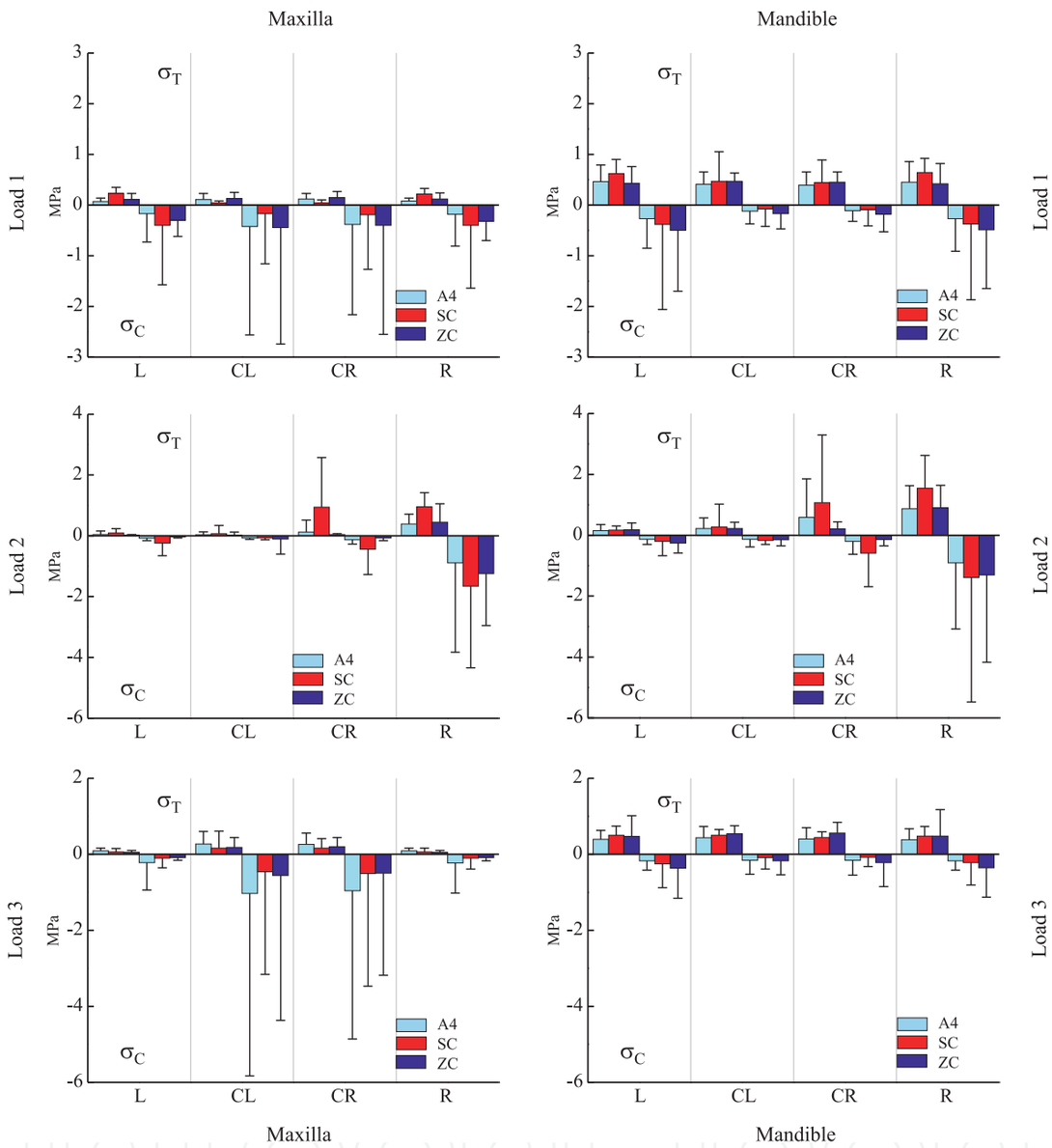

Fig. 10. Principal stress measures (σ_C compressive and σ_T tensile) at the trabecular bone-implant interfaces for implants in A4 (Allon4, light blue bars), SC (SynCone-based, red bars), and ZC (Zero Cantilever, violet bars) restorations, in maxilla (on the left) and mandible (on the right). Average (bars) and peak (lines) values (L: left implant; CL: central-left implant; CR: central-right implant; R: right implant)

edentulous maxilla treated by ZC, posterior short implants transferred the greatest amount of the full-mouth-biting load (mesial P_c was smaller than the distal's of about 50-60%), whereas the frontal load mainly moved towards the bone through the mesial implants (distal P_c was smaller than the mesial's of about 40%). In mandible rehabilitated through the ZC system, both Load 1 and Load 3 were significantly transferred by mesial implants (distal P_c was smaller than the mesial's of about 20%), with transmission mechanisms quite similar to those

induced by A4 and SC in maxilla under Load 3, and with values of mesial P_c slightly higher (about 25%) than those obtained with SC and A4.
Since the different transmission features exhibited by the three techniques when applied in maxilla and mandible, different patterns of the principal stress measures were induced. Under Load 1 and Load 3 and in cortical bone, tensile and compressive stress measures in mandible were greater than in maxilla, whereas they were almost similar for Load 2. Opposite evidences were highlighted at the trabecular peri-implant regions. Moreover, A4 generally produced peaks and mean values of the compressive stresses in distal cortical bone (both mandibular and maxillary) smaller (up to 40-50%) with respect to SC and comparable with ZC. On the contrary, under Load 1 and Load 3, A4 gave rise to values of $\|\sigma_C\|$ at the mesial trabecular peri-implant regions in maxilla higher (up to 90-100% with respect to SC) than those induced by the other techniques. Furthermore, the tilted implants in A4 induced at the crestal bone regions values of the tensile stress σ_T higher (up to 180-200%) than SC and of the same order of magnitude with respect to ZC, especially in mandible.
Physiological limits previously introduced were never reached in cortical bone. On the contrary, the bone strength value for cancellous bone (about 5 MPa) was slightly exceeded in compression for A4 and SC: at the A4's mesial implants in maxilla under the frontal load, and at the SC's right implant in mandible under the cantilever load.

4. Discussion

Proposed numerical results, obtained via three-dimensional finite-element analyses, clearly proved that the four-implant-supported full-arch prostheses based on Allon4 (A4) and SynCone (SC) concepts exhibit very different stress-based biomechanical behavior, as well as different loading transmission characteristics when applied in maxillary and mandibular jaw. Such an evidence was confirmed also in the case of a novel non-conventional approach, based on the use of short implants placed at the posterior molar regions (Zero Cantilever, ZC), in order to minimize the cantilever length. Numerical investigations accounted for functioning implants by modeling crestal bone loss after a healing and loading period. The temporomandibular joints and the loading-dependent muscle-bone static interactions were also modelled in mandible.
Simulation results highlighted that the local bone-implant biomechanical interactions as well as the overall performance of the rehabilitative techniques were mainly dependent on: cantilever length, implant design concepts and crestal positioning (highly affecting the bone-loss level at the implant necks), implant tilt and mutual distances between implant axes, patient-dependent morphology and mechanical properties of bone tissues. Moreover, mutual effects of cantilever and crestal bone geometry were proved to be strongly related to the type of both load and jaw.
In the case of a full-mouth-biting load (Load 1), the influence of the cantilever length was prevailing and the use of distal tilted long implants in A4 (Nobel Biocare implants) or posterior vertical short implants in ZC (Ankylos type) induced smaller overloading risks (mainly in compression) and more uniform stress distributions on bone than the distal vertical implants employed in SC (Ankylos). On the contrary, as a consequence of the reduced level of crestal bone loss induced by the Ankylos devices in SC, mesial implants exhibited opposite comparative results. It is worth pointing out that, although mesial implants in ZC were the same as in SC, they induced compressive stress performance almost comparable with A4. In fact, due to the use of short posterior implants and since the values of L_2 (namely, the distance between the distal implants, see Table 1 and Fig. 2), basic statics allows to show that benefits

associated with platform switching were partially compensated by the different loading partition of ZC, resulting in load components transmitted through the ZC's mesial implants higher with respect to SC (see Fig. 8). Due to the different bone quality and morphology, the greatest overloading risks under Load 1 were computed at the cortical bone-implant interfaces in mandible (for distal implants) and at the trabecular bone in maxilla (for mesial implants), both in compression. Maxillary stress peaks at the trabecular peri-implant regions, as experienced also for the frontal load (Load 3), can be mainly associated to the bone morphology. In fact, due to the thin cancellous layer separating implants and cortical bone at the nasal cavity, high mesial compressive states were generated near the in-bone implant ends (see Fig. 6). This effect reduced when the SC system was employed, because of the more favourable loading partition mechanisms in mesial region with respect to both A4 and ZC (see Fig. 8a).

Under the cantilever load (Load 2), that was proved to be the most dangerous and unbalanced condition, the main influence on the stress-based performance was again related to the cantilever length. Accordingly, the use of tilted implants in A4, reducing the cantilever, allowed to obtain also in this case a loading partition better than SC and smaller risks of bone overload (mainly in compression). Good partition features were also computed for ZC but, since the short length of the posterior implants, compressive stresses at the cortical bone were greater then those of both A4 and SC (although within physiological limits).

As a matter of fact, Load 1 and Load 2 activated the implant-to-bone transfer of mainly intrusive loading components, as directly proportional to the overall load acting upon the bar. In the first case, all implants were involved in such a transfer mechanism and distal implants transferred load components directly depending on the cantilever length as well as on the values of L_1 and L_2 (see Table 1). In the second case (cantilever load), only one or at most two implants were mainly acted upon by an intrusive component (namely, the right implant and at most the mesial-right one, Fig. 8), whereas implants on the opposite side (on the left) were practically unloaded. A frontal load (Load 3) did not activate cantilever mechanisms. Therefore, main effects can be associated to platform switching and implant positioning. In this case the highest stress peaks were computed at the cortical bone in mandible and at the cancellous bone in maxilla. Under the frontal load, the transfer characteristics of the conventional approaches (A4 and SC) were proved to be strongly different in lower and upper arches, A4 resulting better in mandible and worse in maxilla than SC. On the contrary, the loading partition achieved by the non-conventional ZC system was weakly affected by the jaw type, resulting better than A4 in maxilla and the worst in mandible. These evidences can be strictly related to the distances between mesial and distal implants (namely, L_1 and L_2, Fig. 2), that depend on both treatment type and jaw morphology. In fact, when an intrusive force component acted upon the prosthetic bar at the middle of the central span (Load 3), the load was statically transferred towards the bone mainly by intrusive actions upon the mesial implants and by extrusive upon the distal ones. In agreement with basic statics, when L_1 reduced (passing from mandibular to maxillary applications) intrusive forces acting upon the mesial implants increased and distal extrusive ones reduced, modifying the loading partition performance. Moreover, when the difference $(L_2 - L_1)$ increased (*e.g.*, passing from SC to A4, or from A4 to ZC) distal extrusive actions further reduced, producing an additional contribution towards a non-homogeneous loading partition.

As presented results have proved, tilted implants in A4 or short posterior implants in ZC may induce tensile stresses greater than SC at the cortical bone, mainly in mandible because of the crestal bone morphology. Nevertheless, the localization of bone areas subjected to these

traction states was strongly dependent on the loading type. In fact, when mainly intrusive components loaded tilted distal or posterior short implants (namely, Load 1 and Load 2), prevailing compressive states were induced at the distal side of the cortical bone-implant interface and prevailing bone tractions appeared at the opposite side. Conversely, when mainly extrusive loading components were considered on tilted or posterior implants (Load 3), tractions were essentially localized at the distal side of the peri-implant cortical region and compressive stresses arose at the mesial side.

Proposed numerical findings confirm that a rehabilitative full-arch technique should be chosen and/or designed by bearing in mind that the loading transmission features and the risks of bone resporption activation are strongly affected by cantilever configurations, as well as by morphological and mechanical bone properties. In detail, in agreement with many clinical (Aparicio et al., 2001; Calandriello & Tomatis, 2005; Capelli et al., 2007; Del Fabbro et al., 2010; Krekmanov et al., 2000; Malò et al., 2005; Sertgöz & Güvener, 1996; Shackleton et al., 1994; Testori et al., 2008; White et al., 1994), photoelastic (Begg et al., 2009), and numerical (Bellini, 2009; Bonnet et al., 2009; Carvalho Silva et al., 2010; Zampelis et al., 2007) evidences, an higher distal cantilever length has been proved to induce higher and dangerous stress concentrations on bone, mainly at the distal peri-implant regions. Therefore, proposed results confirm that the biomechanical rationale related to the use of tilted distal implants is effective for reducing cantilever mechanisms and generally for inducing more favourable load transmission characteristics. Nevertheless, as a complementary and novel indication, present results have clearly proved that tilted implants can produce high tensile stress concentrations at distal peri-implant regions, inducing high risks of an ineffective osseous integration process and of local bone damage (bone is most resistant against compressive stress and 30% less against the tensile actions, Guo (2001)). The localization at the cortical bone-implant interfaces of these traction states was proved to be strongly dependent on the loading type. In agreement with previous researches (Baggi et al., 2008b; Begg et al., 2009; Carvalho Silva et al., 2010; Chun et al., 2006; Clelland et al., 1993; Petrie & Williams, 2005; Van Staden et al., 2006), present numerical simulations have also confirmed that possible bone overloads can affect cortical regions around the implant necks, mainly in compression. In addition, present numerical findings have shown that for implants mesially placed in maxillary arch, overloading risks in trabecular bone are mainly depending on jaw morphology and they proportionally increase with the in-bone implant depth. Moreover, in agreement with numerical results proposed by Maeda et al. (2007) and by Baggi et al. (2008a;b), the biomechanical stress-based performance of a rehabilitative technique and its long-term effectiveness can be significantly improved, especially for loads that does not induce significant cantilever effects (as for purely frontal loads), if crestal bone loss is effectively counteracted. As a further novel contribution, proposed numerical analyses have showed that the use of non-conventional short implants based on platform switching concepts and vertically placed in the posterior region, allow both to vanish cantilever length and to obtain stress distributions and loading transmission features fully comparable (sometimes better) than the Allon4-based conventional technique. Accordingly, such an approach can be retained as an effective alternative to the actual clinical protocols, although it could be enhanced by choosing suitable values of parameters L_1 and L_2, consistent with patient-specific bone morphology and allowing for optimal bone-implant biomechanical interactions.

It is worth pointing out that, in a number of recent numerical researches the influence of crestal bone loss in functioning implants, of detailed geometrical modeling for lower and upper jaws, as well as of muscle-bone static interactions and temporomandibular

articulation have been disregarded (*e.g.*, Baggi et al., 2008b; Bellini, 2009; Bonnet et al., 2009; Carvalho Silva et al., 2010; Chun et al., 2006; Kitagawa et al., 2005; Maeda et al., 2007; Petrie & Williams, 2005; Van Staden et al., 2006; Zampelis et al., 2007). In the present study, although different crestal bone loss configurations were considered, the ideal condition of a complete osseous integration between implants and bone was assumed. Furthermore, stress analyses were performed by assuming static loads and, in agreement with modeling approaches available in literature (Lekholm & Zarb, 1985; Trainor et al., 1995), by including temporomandibular joints and muscular forces on mandible. As far as the mechanical behavior of bone is concerned, living tissues were modelled as isotropic linearly elastic materials, distinguishing two homogeneous material volumes describing the trabecular and cortical regions. These assumptions do not exactly represent actual clinical scenarios because of: possible osseointegration defects; different loading distributions due to patient-dependent functional and aesthetics prosthetic elements; much more complex and time-dependent both functional forces and muscular effects; anisotropic, non-homogeneous, non-linear and inelastic response of living tissues. Nevertheless, in agreement with a number of well-established numerical results (*e.g.*, Baggi et al., 2008a;b; Beek et al., 2000; Bellini, 2009; Bonnet et al., 2009; Carvalho Silva et al., 2010; Chun et al., 2006; Kitagawa et al., 2005; Maeda et al., 2007; Petrie & Williams, 2005; Sertgöz & Güvener, 1996; Trainor et al., 1995; Van Staden et al., 2006; White et al., 1994; Zampelis et al., 2007), the present assumptions can be considered as effective and consistent in a computational sense, in order to deduce significant and clinically useful indications. Accordingly, proposed fully three-dimensional simulation approach can be considered as an accurate and effective tool for stress-based comparative assessment of full-arch rehabilitations.

With the aim to enhance the present finite-element formulation, next studies will be devoted to model the bone as a non-linearly anisotropic, viscous and non-homogeneous regenerative tissue, that responds to stress by resorption or regeneration under time-dependent muscular and external loads.

5. Concluding remarks

Within the limitations of this study, proposed three-dimensional finite-element simulations proved that the "Allon4" and "SynCone"-based full-arch rehabilitative systems, supported by four endosseous implants, induced load transmission mechanisms and bone overloading risks highly different when mandibular and maxillary applications were compared. Simulation results were obtained through detailed numerical models of both lower and upper jaw, and were analyzed by introducing meaningful performance indexes and local stress measures. The coupled influences of several biomechanical factors were clearly highlighted, indicating that the prevailing effects are related to the cantilever length, the implant design concepts and positioning, the bone morphology and its mechanical properties. Stress concentrations occurred in compression at the implant necks and, depending on implant length and jaw morphology, at the in-bone implant ends. The reduction of the distal cantilever by employing tilted implants (Allon4 system) allowed to enhance the loading distribution and to reduce the risks of bone resorption activation at the distal peri-implant regions. Nevertheless, tilted distal implants induced on cortical bone and for all loads analyzed in this study higher tensile stresses than vertical distal implants, producing higher risks of non-effective crestal osseous integration and of bone damage. The localization of these traction states was proved to be mainly dependent on the loading type, and their intensity was greatly affected by crestal bone quantity and quality. When implants based on a platform-switching configuration

and subcrestal positioning were considered (Ankylos implants in SynCone-based system), since the reduced level of crestal bone loss, more favourable and homogeneous stress distributions were computed at the implant necks and at the trabecular bone, such an effect resulting prevailing for mesial implants and when the load did not significantly activate cantilever transmission mechanisms. Therefore, although both systems seemed to ensure stress levels physiologically admissible in both mandibular and maxillary rehabilitations, proposed numerical results clearly indicated that each technique has both benefits and drawbacks, essentially as a result of mutual coupling between cantilever mechanisms and cratering effects.

Finally, in this study the possible use of a non-conventional full-arch rehabilitative system, based on four vertical implants consistent with platform switching concepts, has been also investigated. Following such an approach, two commercially-available mesial implants are combined with two non-conventional short implants placed at the posterior molar regions. In this way cantilever length is minimized (up to zero, if the patient-dependent bone quality and quantity in that region permit it) and, since also the platform-switching effects, both transmission mechanisms and overloading risks can result comparable or better than other well-established conventional techniques. Accordingly, such an approach can be surely considered as an effective and reliable clinical alternative to available actual protocols.

6. References

Abboud, M.; Koeck, B.; Stark, H.; Wahl, G.; Paillon, R. (2005). Immediate loading of single tooth implants in the posterior region. *International Journal of Oral Maxillofacial & Implants*, Vol. 20, No. 1, February 2005, 61–68, ISSN 0882-2786

Al-Nawas, B.; Wegener, J.; Bender, C.; Wagner, W. (2004). Critical soft tissue parameters of the zygomatic implant. *Journal of Clinical Periodontology*, Vol. 31, No. 7, July 2004, 497–500, ISSN 0303-6979

Aparicio, C.; Perales, P.; Rangert, B. (2001). Tilted implants as an alternative to maxillary sinus grafting: A clinical, radiologic, and periotest study. *Clinical Implant Dentistry and Related Research*, Vol. 3, No. 1, January 2001, 39–49, ISSN 1708-8208

Baggi, L.; Cappelloni, I.; Di Girolamo, M.; Maceri, F.; Vairo, G. (2008). The influence of implant diameter and length on stress distribution of osseointegrated implants related to crestal bone geometry: A three-dimensional finite element analysis. *Journal of Prosthetic Dentistry*, Vol. 100, No. 6, December 2008, 422–431, ISSN 0022-3913

Baggi, L.; Cappelloni, I.; Maceri, F.; Vairo, G. (2008) Stress-based performance evaluation of osseointegrated dental implants. *Simulation Modelling Practice & Theory*, Vol. 16, No. 8, September 2008, 971–987, ISSN 1569-190X

Bayer, S.; Stark, H.; Mues, S.; Keilig, L.; Schrader, A.; Enkling, N. (2009). Retention force measurement of telescopic crowns. *Clinical Oral Investigations*, Vol. 14, No. 5, 607–611, ISSN 1432-6981

Beek, M.; Koolstra, J.H.; Van Ruijven, L.J.; Van Eijden, T.M.G.J. (2000). Three-dimensional finite element analysis of the human temporomandibular joint disc. *Journal of Biomechanics*, Vol. 33, No. 3, March 2000, 307–316, ISSN 0021-9290

Begg, T.; Geerts, G.A.; Gryzagoridis J. (2009). Stress patterns around distal angled implants in the all-on-four concept configuration. *International Journal of Oral Maxillofacial & Implants*, Vol. 24, No. 4, July-August 2009, 663–671, ISSN 0882-2786

Bellini, C.; Romeo, D.; Galbusera, F.; Agliardi, E.; Pietrabissa, R.; Zampelis, A.; Francetti, L. (2009). A finite element analysis of tilted versus non-tilted implant configurations

in the edentulous maxilla. *International Journal of Prosthodontics*, Vol. 22, No. 2, March-April 2009, 155–157, ISSN 0893-2174

Bocklage, R. (2002). Rehabilitation of the edentulous maxilla and mandible with fixed implant-supported restorations applying immediate functional loading: A treatment concept. *Implant Dentistry*, Vol. 11, No. 2, June 2002, 154–158, ISSN 1056-6163

Bonnet, A.S.; Postaire, M.; Lipinski, P. (2009). Biomechanical study of mandible bone supporting a four-implant retained bridge: finite element analysis of the influence of bone anisotropy and foodstuff position. *Medical Engineering & Physics*, Vol. 31, No. 7, September 2009, 806–815, ISSN 1350-4533

Brunski, J.B. (1997). Biomechanics of dental implants. In: *Implants in dentistry: Essentials of endosseous implants for maxillofacial reconstruction*. Block, M.S.; Kent, J.N.; Guerra, L.R. (Eds.), 63–71, Saunders, ISBN 0721621740, Philadelphia

Calandriello, R. & Tomatis, M. (2005). Simplified treatment of the atrophic posterior maxilla via immediate/early function and tilted implants: A prospective 1-year clinical study. *Clinical Implant Dentistry and Related Research*, Vol. 7, No. s1, s1–s12, ISSN 1708-8208

Capelli, M.; Zuffetti, F.; Del Fabbro, M.; Testori, T. (2007). Immediate rehabilitation of the completely edentulous jaw with fixed prostheses supported by either upright or tilted implants: A multicenter clinical study. *International Journal of Oral Maxillofacial & Implants*, Vol. 22, No. 4, July-August 2007, 639–644, ISSN 0882-2786

Carter, D.R.; Van Der Meulen, M.C.; Beaupré, G.S. (1996). Mechanical factors in bone growth and development. *Bone*, Vol. 18, No. 1 Suppl., 5S–10S, ISSN 8756-3282

Carvalho Silva, G.; Mendonça, J.A.; Randazzo Lopez, L.; Landre, J. (2010). Stress patterns on implants in prostheses supported by four or six implants: A three-dimensional finite element analysis. *International Journal of Oral Maxillofacial & Implants*, Vol. 25, No. 2, March 2010, 239–246, ISSN 0882-2786

Chun, H.J.; Shin, H.S.; Han, C.H.; Lee, S.H. (2006) Influence of implant abutment type on stress distribution in bone under various loading conditions using finite element analysis. *International Journal of Oral Maxillofacial & Implants*, Vol. 21, No. 2, March-April 2006, 195–202, ISSN 0882-2786

Chung, D.M.; Oh, T.J.; Lee, J.; Misch, C.E.; Wang, H.L. (2007). Factors affecting late implant bone loss: A retrospective analysis. *International Journal of Oral & Maxillofacial Implants*, Vol. 22, No. 1, January-February 2007, 117–126, ISSN 0882-2786

Clelland, N.L.; Gilat, A.; McGlumphy, E.A.; Brantley, W.A. (1993). A photoelastic and strain gauge analysis of angled abutments for an implant system. *International Journal of Oral Maxillofacial & Implants*, Vol. 8, No. 5, ISSN 0882-2786

Degidi, M. & Piattelli, A. (2005). A 7-year follow-up of 93 immediately loaded titanium dental implants. *Journal of Oral Implantology*, Vol. 31, No. 1, February 2005, 25–31, ISSN 0160-6972

Degidi, M.; Piattelli, A.; Shibli, J.A.; Strocchi, R.; Iezzi, G. (2009). Bone formation around a dental implant with a platform switching and another with a TissueCare Connection. A histologic and histomorphometric evaluation in man. *Titatnium*, Vol. 1, No. 1, 8–15, ISSN 1946-0155

Del Fabbro, M.; Bellini, C.M.; Romeo, D.; Francetti, L. (2010). Tilted implants for the rehabilitation of edentulous jaws: A systematic review. *Clinical Implant Dentistry and Related Research*, doi:10.1111/j.1708-8208.2010.00288.x, ISSN 1708-8208

Devlin, H.; Horner, K.; Ledgerton, D. (1998). A comparison of maxillary and mandibular bone mineral densities. *Journal of Prosthetic Dentistry*, Vol. 79, No. 3, March 1998, 323–327, ISSN 0022-3913

Drago, C.J. (1992). Rates of osseointegration of dental implants with regard to anatomical location. *Journal of Prosthodontics*, Vol. 1, No. 1, September 1992, 29–31, ISSN 1532-849X

Eccellente, T.; Piombino, M.; Piattelli, A.; Perrotti, V.; Iezzi, G. (2010). A new treatment concept for immediate loading of implants inserted in the edentulous mandible. *Quintessence International*, Vol. 41, No. 6, June 2010, 489–495, ISSN 0033-6572

Eckert, S.E. & Wollan, P.C. (1998). Retrospective review of 1170 endosseous implants placed in partially edentulous jaws. *Journal of Prosthetic Dentistry*, Vol. 79, No. 4, April 1998, 415–421, ISSN 0022-3913

Ferreira, E.J.; Kuabara, M.R.; Gulinelli, J.L. (2010). "All-on-four" concept and immediate loading for simultaneous rehabilitation of the atrophic maxilla and mandible with conventional and zygomatic implants. *British Journal of Oral and Maxillofacial Surgery*, Vol. 48, No. 3, April 2010, 218–220, ISSN 0266-4356

Ganeles, J.; Rosenberg, M.M.; Holt, R.L.; Reichmann, L.H. (2001). Immediate loading of implants with fixed restorations in the completely edentulous mandible: Report of 27 patients from private practice. *International Journal of Oral & Maxillofacial Implants*, Vol. 16, No. 3, May-June 2001, 418–426, ISSN 0882-2786

Guo, X.E. (2001). Mechanical properties of cortical and cancellous bone tissue. In: *Bone Mechanics Handbook* (2nd ed.). Cowin, S.C. (Ed.), 10.1–10.23, CRC Press, ISBN 0849391172, Boca Raton

Irving, J.T. (1970). Factors concerning bone loss associated with periodontal disease. *Journal of Dental Research*, Vol. 49, No. 2, 262–267, ISSN 0022-0345

Keller, E.E.; Van Roekel, N.B.; Desjardins, R.P.; Tolman, D.E. (1987). Prosthetic-surgical reconstruction of the severely resorbed maxilla with iliac bone grafting and tissue-integrated prostheses. *International Journal of Oral & Maxillofacial Implants*, Vol. 2, No. 3, Summer 1987, 155–165, ISSN 0882-2786

Khatami, A.H. & Smith, C.R. (2008). All-on-Four immediate function concept and clinical report of treatment of an edentulous mandible with a fixed complete denture and milled titanium framework. *Journal of Prosthondontics*, Vol. 17, No. 1, January 2008, 47–51, ISSN 1532-849X

Kitagawa, T.; Tanimoto, Y.; Nemoto, K.; Aida, M. (2005). Influence of cortical bone quality on stress distribution in bone around dental implant. *Dental Materials Journal*, Vol. 24, 219–224, ISSN 0287-4547

Krekmanov, L.; Kahn, M.; Rangert, B.; Lindström, H. (2000). Tilting of posterior mandibular and maxillary implants for improved prosthesis support. *International Journal of Oral Maxillofacial & Implants*, Vol. 15, No. 3, May-June 2000, 405–414, ISSN 0882-2786

Lazzara, R.J. & Porter, S.S. (2006). Platform switching: A new concept in implant dentistry for controlling postrestorative crestal bone levels. *International Journal of Periodontics & Restorative Dentistry*, Vol. 26, No. 1, February 2006, 9–17, ISSN 0198-7569

Lekholm, U. & Zarb, G.A. (1985). Patient selection and preparation. In: *Tissue-integrated prostheses: Osseointegration in clinical dentistry*. Brånemark, P.I.; Zarb, G.A.; Albrektsson, T. (Eds.), 109–209, Quintessence, ISBN 0867151293, Chicago

Lekholm, U.; Gunne, J.; Henry, P.; Higuchi, K.; Linden, U.; Bergstrom, C. et al. (1999). Survival of the Brånemark implant in partially edentulous jaws: A 10-year prospective

multicenter study. *International Journal of Oral & Maxillofacial Implants*, Vol. 14, No. 5, September-October 1999, 639–645, ISSN 0882-2786

Lemon, J.E. & Dietsh-Misch, F. (2007). Biomaterials for dental implants. In: *Contemporary implant dentistry* (3rd ed.). Misch, C.E. (Ed.), 271–302, Mosby, ISBN 0323043739, St. Louis

Lòpez-Marì, L.; Calvo-Guirado, J.L.; Martín-Castellote, B.; Gomez-Moreno, G.; Lòpez-Marì, M. (2009). Implant platform switching concept: An updated review. *Medicina Oral, Patología Oral y Cirugía Bucal*, Vol. 14, No. 9, September 2009, e450–e454, ISSN 1698-6946

Maceri, F.; Martignoni, M.; Vairo, G. (2007). Mechanical behaviour of endodontic restorations with multiple prefabricated posts: A finite-element approach. *Journal of Biomechanics*, Vol. 40, No. 11, 2386–2398, ISSN 0021-9290

Maceri, F.; Martignoni, M.; Vairo, G. (2009). Optimal mechanical design of anatomical post-systems for endodontic restoration. *Computer Methods in Biomechanics and Biomedical Engineering*, Vol. 12, No. 1, February 2009, ISSN 1025-5842

Maeda, Y.; Miura, J.; Taki, I.; Sogo, M. (2007). Biomechanical analysis on platform switching: Is there any biomechanical rationale? *Clinical Oral Implants Research*, Vol. 18, No. 5, October 2007, 581–584, ISSN 1600-0501

Mailath-Pokorny, G. & Solar, P. (1996). Biomechanics of endosseous implants. In: *Endosseous Implants: Scientific and Clinical Aspects*. Watzek, G. (Ed.), 291–318, Quintessence Publishing, ISBN 0867153024, Chicago

Malò, P.; Rangert, B.; Nobre, M. (2005). All-on-4 immediate-function concept with Brånemark system implants for completely edentulous maxillae: A 1-year retrospective clinical study. *Clinical Oral Implants Research*, Vol. 7, No. s1, June 2005, s88–s94, ISSN 1600-0501

Natali, A.N.; Hart, R.T.; Pavan, P.G.; Knets, I. (2003). Mechanics of bone tissue. In: *Dental Biomechanics*. Natali, A.N. (Ed.), 1–19, Taylor & Francis, ISBN 0415306663, London

Papadopoulos, M.A. & Tarawneh, F. (2007). The use of miniscrew implants for temporary skeletal anchorage in orthodontics: A comprehensive review. *Oral Surgery, Oral Medicine, Oral Pathology, Oral Radiology & Endododontics*, Vol.103, No. 5, May 2007, e6–e15, ISSN 1079-2104

Petrie, C.S. & Williams, J.L. (2005). Comparative evaluation of implant designs: Influence of diameter, length, and taper on strains in the alveolar crest. A three-dimensional finite element analysis. *Clinical Oral Implants Research*, Vol. 16, No. 4, August 2005, 486–494, ISSN 0905-7161

Piattelli, A.; Scarano, A.; Piattelli, M. (1996). Microscopical aspects of failure in osseointegrated dental implants: A report of five cases. *Biomaterials*, Vol. 17, No. 12, June 1996, 1235–1241, ISNN 0142-9612

Portmann, M. & Glauser R. (2006). Report of a case receiving full-arch rehabilitation in both jaws using immediate implant loading protocols: A 1-year resonance frequency analysis follow-up. *Clinical Implant Dentistry and Related Research*, Vol. 8, No. 1, March 2006, 25–31, ISSN 1708-8208

Puig, C.P. (2010). A retrospective study of edentulous patients rehabilitated according to the 'all-on-four' or the 'all-on-six' immediate function concept using flapless computer-guided implant surgery. *European Journal of Oral Implantology*, Vol. 3, No. 2, Summer 2010, 155–163, ISSN 1756-2406

Renouard, F.; Nisand, D. (2005). Short implants in the severely resorbed maxilla: A 2-year retrospective clinical study. *Clinical Implant Dentistry and Related Research*, Vol. 7, No. s1, June 2005, s104–s110, ISSN 1708-8208

Romanos, G.E. (2004). Present status of immediate loading of oral implants. *Journal of Oral Implantology*, Vol. 30, No. 3, June 2004, 189–197, ISSN 0160-6972

Romeo, E.; Chiapasco, M.; Ghisolfi, M.; Vogel, G. (2002). Long-term clinical effectiveness of oral implants in the treatment of partial edentulism. Seven-year life table analysis of a prospective study with ITI dental implants system used for single-tooth restorations. *Clinical Oral Implants Research*, Vol. 13, No. 2, April 2002, 133–143, ISSN 1600-0501

Roos-Jansåker, A.M.; Lindahl, C.; Renvert, H.; Renvert, S. (2006). Nine- to fourteen-year follow-up of implant treatment. Part I: Implant loss and associations to various factors. *Journal of Clinical Periodontology*, Vol. 33, No. 4, April 2006, 283–289, ISSN 0303-6979

Sertgöz, A. & Güvener, S. (1996). Finite element analysis of the effect of cantilever and implant length on stress distribution in an implant-supported fixed prosthesis. *Journal of Prosthetic Dentistry*, Vol. 76, No. 2, August 1996, 165–169, ISSN 0022-3913

Shackleton, J.L.; Carr, L.; Slabbert, J.C.; Becker, P.J. (1994). Survival of fixed implant-supported prostheses related to cantilever lengths. *Journal of Prosthetic Dentistry*, Vol. 71, No. 1, January 1994, 23–26, ISSN 0022-3913

Shin, Y.K.; Han, C.H.; Heo, S.J.; Kim, S.; Chun, H.J. (2006). Radiographic evaluation of marginal bone level around implants with different neck designs after 1 year. *International Journal of Oral Maxillofacial & Implants*, Vol. 21, No. 5, September-October 2006, 789–794, ISSN 0882-2786

Tatum, H. (1986). Maxillary and sinus implant reconstruction. *Dental Clinics of North America*, Vol. 30, No. 2, 207–229, ISSN 0011-8532

Testori, T.; Del Fabbro, M.; Capelli, M.; Zuffetti, F.; Francetti, L.; Weinstein; R.L. (2008). Immediate occlusal loading and tilted implants for the rehabilitation of the atrophic edentulous maxilla: 1-year interim result of a multicenter prospective study. *Clinical Oral Implants Research*, Vol. 19, No. 3, March 2008, 227–232, ISSN 1600-0501

Tonetti, M.S. (1999). Determination of the success and failure of root-form osseointegrated dental implants. *Advances in Dental Research*, Vol. 13, No. 1, June 1999, 173–180, ISSN 0895-9374

Trainor, P.G.; McLachlan, K.R.; McCall, W.D. (1995). Modelling of forces in the human masticatory system with optimization of the angulations of the joint loads. *Journal of Biomechanics*, Vol. 28, No. 7, July 1995, 829–843, ISSN 0021-9290

Van Staden, R.C.; Guan, H.; Loo, Y.C. (2006). Application of the finite element method in dental implant research. *Computer Methods in Biomechanics and Biomedical Engineering*, Vol. 9, No. 4, August 2006, 257–270, ISSN 1025-5842

Weyant, R. (2003). Short-term clinical success of root-form titanium implant systems. *Journal of Evidence-Based Dental Practice*, Vol. 3, No. 3, September 2003, 127–130, ISSN 1532-3382

White, S.N.; Caputo, A.A.; Anderkvist, T. (1994). Effect of cantilever length on stress transfer by implant-supported prostheses. *Journal of Prosthetic Dentistry*, Vol. 71, No. 5, May 1994, 493–499, ISSN 0022-3913

Wostmann, B.; Balkenhol, M.; Weber, A.; Ferger, P.; Rehmann, P. (2007). Long-term analysis of telescopic crown retained removable partial dentures: Survival and need for maintenance. *Journal of Dentistry*, Vol. 35, No. 12, December 2007, 939–945, ISSN 0300-5712

Wostmann, B.; Balkenhol, M.; Kothe, A.; Ferger, P. (2008). Dental impact on daily living of telescopic crown-retained partial dentures. *International Journal of Prosthodontics*, Vol. 21, No. 5, September-October 2008, 419–421, ISSN 0893-2174

Zampelis, A.; Rangert, B.; Heijl, L. (2007). Tilting of splinted implants for improved prosthodontic support: A two-dimensional finite element analysis. *Journal of Prosthetic Dentistry*, Vol. 97, No. 6 (s1), June 2007, s35-s43, ISSN 0022-3913

Zienkiewicz, O.C. & Zhu, J.Z. (1987). A simple error estimator and adaptive procedure for practical engineering analysis. *International Journal for Numerical Methods in Engineering*, Vol. 24, No. 2, Febraury 1987, 337–357, ISSN 0029-5981

Zienkiewicz, O.C. & Taylor R.L. (1998). *The Finite Element Method*, 6th ed., Elsevier Buttherworth-Heinemann, ISBN 0750663219, Burlington

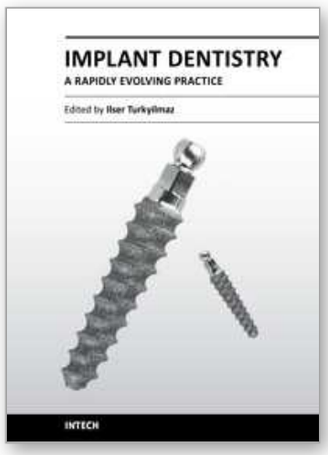

Implant Dentistry - A Rapidly Evolving Practice

Edited by Prof. Ilser Turkyilmaz

ISBN 978-953-307-658-4
Hard cover, 544 pages
Publisher InTech
Published online 29, August, 2011
Published in print edition August, 2011

Implant dentistry has come a long way since Dr. Branemark introduced the osseointegration concept with endosseous implants. The use of dental implants has increased exponentially in the last three decades. As implant treatment became more predictable, the benefits of therapy became evident. The demand for dental implants has fueled a rapid expansion of the market. Presently, general dentists and a variety of specialists offer implants as a solution to partial and complete edentulism. Implant dentistry continues to evolve and expand with the development of new surgical and prosthodontic techniques. The aim of Implant Dentistry - A Rapidly Evolving Practice, is to provide a comtemporary clinic resource for dentists who want to replace missing teeth with dental implants. It is a text that relates one chapter to every other chapter and integrates common threads among science, clinical experience and future concepts. This book consists of 23 chapters divided into five sections. We believe that, Implant Dentistry: A Rapidly Evolving Practice, will be a valuable source for dental students, post-graduate residents, general dentists and specialists who want to know more about dental implants.

INTECH
open science | open minds

InTech Europe
University Campus STeP Ri
Slavka Krautzeka 83/A
51000 Rijeka, Croatia
Phone: +385 (51) 770 447
Fax: +385 (51) 686 166
www.intechopen.com

InTech China
Unit 405, Office Block, Hotel Equatorial Shanghai
No.65, Yan An Road (West), Shanghai, 200040, China
中国上海市延安西路65号上海国际贵都大饭店办公楼405单元
Phone: +86-21-62489820
Fax: +86-21-62489821

IntechOpen